

LA-8583-PR

Progress Report

C.2

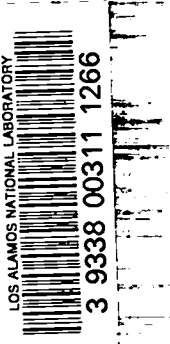
2

**Armor Defeat Mechanisms,
Alternative Materials Selection**

May—September 1980



University of California



DO NOT CIRCULATE

PERMANENT RETENTION

REQUIRED BY CONTRACT



LOS ALAMOS SCIENTIFIC LABORATORY

Post Office Box 1663 Los Alamos, New Mexico 87545

An Affirmative Action/Equal Opportunity Employer

5.9
A

The previous report in this series, unclassified,
is LA-8413-PR.

This report was not edited by the Technical
Information staff.

This work was supported by the Air Force
Armament Training Laboratory.

DISCLAIMER

This report was prepared as an account of work sponsored by an agency of the United States Government. Neither the United States Government nor any agency thereof, nor any of their employees, makes any warranty, express or implied, or assumes any legal liability or responsibility for the accuracy, completeness, or usefulness of any information, apparatus, product, or process disclosed, or represents that its use would not infringe privately owned rights. Reference herein to any specific commercial product, process, or service by trade name, trademark, manufacturer, or otherwise, does not necessarily constitute or imply its endorsement, recommendation, or favoring by the United States Government or any agency thereof. The views and opinions of authors expressed herein do not necessarily state or reflect those of the United States Government or any agency thereof.

**UNITED STATES
DEPARTMENT OF ENERGY
CONTRACT W-7405-ENG. 36**

LA-8583-PR
Progress Report

UC-25
Issued: October 1980

Armor Defeat Mechanisms, Alternative Materials Selection

May—September 1980

Compiled by

J. M. Dickinson

Contributors

P. E. Armstrong	J. F. Muller
K. V. Davidson	J. A. O'Rourke
C. F. Frantz	R. D. Reiswig
S. S. Hecker	A. D. Rollett
C. A. Javorsky	D. J. Sandstrom
T. I. Jones	W. H. Zimmer
C. W. Mautz	

LOS ALAMOS NATL. LAB. LIBS.

3 9338 00311 1266



ARMOR DEFEAT MECHANISMS,
ALTERNATIVE MATERIALS SELECTION

May - September 1980

Compiled by
J. M. Dickinson

ABSTRACT

Materials characterization and selection studies on liner materials for shaped charge projectiles are presented. Mechanical property measurements were made over a strain rate of 10^{-3} to 10^4 s⁻¹. Results of compression tests, biaxial stretching tests, tensile tests, and Taylor anvil tests are included. Microstructural analysis and trace element chemical analysis were reported for most of the materials and their relationships to the ductility and fracture behavior of the materials are discussed.

1. INTRODUCTION

We originally planned to examine the properties of six different uranium materials as a function of strain rate during FY 80. The choice of materials selected for these examinations has been changed several times to respond to immediate needs of the general armor defeat mechanism program. This has resulted in characterization of several materials that have been fired as actual liners, rather than the originally selected materials, and could actually increase the utility of the program.

Materials being examined are listed in Table I. The most extensive characterization to date has been done on the first four materials listed in Table I; the other materials are in various stages of processing and testing at this time.

TABLE I
MATERIALS SLATED FOR CHARACTERIZATION DURING FY 80

<u>Material</u>	<u>General Description</u>	<u>Corresponding Mautz Shot No.</u>
U, CM 3 8480	Y-12 fine grained, < 100 ppm carbon	M3-E-4760-4761
U, 69072-	Y-12 run-of-the-mill, typical wrought production uranium	M3-E-4795
U, CMB-6-70227 (*)	LASL as-cast, three castings were made.	M3-E-4763
U, CMB-6-70233		M3-E-4764
U, CMB-6-70234		
U, LA 2233	LASL isotropic fine grained uranium, low carbon	
U, CMB-6-C1-900	LASL cast, extruded, forged and rolled, low carbon	
U, CMB-6-C1-901	LASL cast, extruded, forged and rolled, very low carbon	
U, CMB-6-C1-903	LASL cast and rolled, low carbon	
U-Nb alloy		

(*) Material CMB-6-70227 and 70233 were used for shots number E-4763 and 4764 but the identity of the castings were not kept separate during machining. Since all three castings were made in the same way from the same material, they should be identical. CMB-6-70234 was used for characterization studies.

Additional materials, including alloys of uranium, will be added to this list for evaluation during the next fiscal year. We particularly want to examine uranium alloys having different phases, alloys that do not undergo phase transformations and alloys with better corrosion resistance than pure uranium during FY 81.

Table II contains the results of spectrographic chemical analysis on several of the materials. In general, there were few differences in impurity content and none appeared to explain the behavior of the materials. Results of carbon and hydrogen analysis along with grain size and DPH hardness are shown in Table III for several of the uranium materials. There are significant differences. Analysis are still pending on several samples and will be available soon. The significance of the interstitials will be discussed in more detail later.

The examinations conducted this quarter have included both normal and high strain rate uniaxial and biaxial tensile tests in addition to extensive metallographic studies. These are reported in the following sections.

2. FINE-GRAINED ISOTROPIC URANIUM (LASL MATERIAL LA 2233)

In the last reporting period¹ we presented results from uniaxial tension and uniaxial compression tests at low strain rates and Taylor Anvil tests at high strain rates. We have since prepared compression specimens for the Hopkinson split pressure bar and these will be tested at room temperature using strain rates of 1000 to 5000s⁻¹ during the next reporting period.

Compression tests were conducted on LASL 2233 uranium at elevated temperatures by Robinson, Sherby and Armstrong² in the early 1970's. The results of tests at several different strain rates in the high temperature alpha region (604°C), the beta region (700°C) and the low temperature gamma region (800°C) are shown in Fig. 1. The flow curves are very strain-rate sensitive in all phase regions.

The most striking result is that the beta phase is much stronger than either the alpha or the gamma phases. Since all tests were done in compression, no ductility information was generated.

3. URANIUM CM 3 8480

3.1 Elevated Temperature - High Strain Rate Tensile Studies

Last quarter¹ both normal and high strain rate tensile data at room temperature were reported on this uranium, CM 3 8480; this quarter data has been generated at elevated temperature and high strain rates. The high temperature-high strain rate tests were made on both flat sheet and round button head specimens using our two-inch-gun (TIG) with a projectile velocity of 45 ms⁻¹ resulting in a strain rate of ~ 3000 s⁻¹. A sketch of the apparatus used is shown in Fig. 2. Details of the test were discussed by Franz and Hecker³.

TABLE II
CHEMICAL ANALYSIS OF URANIUM

Element	Y-12 Sheet	CMB-6 Castings		Y-12 Sheet	CMB-6	CMB-6	CMB-6	LASL
	CM 3-8480	70227	70233	69072-27	C1-900	C1-901	C1-903	2233
	ppm	ppm	ppm	ppm	ppm	ppm	ppm	ppm
Li	< 0.2	< 0.2	< 0.2	< 0.2	< 0.2	< 0.2	< 0.2	< 0.1
Mg	50	35	6	6	2-18	6-12	7	< 1
Ca	6	< 6	12	< 6	< 6	< 6	< 6	< 10
Mn	12	12	12	35	6	4-5	7	6
Cu	8	7	10	25	9	5-7	6	6
Nb	< 12	< 35	< 35	< 12	-	-	-	-
Sn	< 1	< 1	< 1	< 1	< 1	< 1	< 1	-
W	< 5	< 6	< 6	< 6	-	-	-	-
Be	< 0.2	< 0.2	< 0.2	< 0.2	< 0.2	< 0.2	< 0.2	< 0.1
Al	30	30	25	13	12-18	6-18	2.5	23
Ti	< 4	< 4	< 4	< 4	-	-	-	-
Fe	70	50	70	120	35-60	25-40	30-35	70
Zn	< 30	< 30	< 30	< 30	< 30	< 30	< 30	-
Mo	4	< 4	< 4	10	< 30	< 30	< 30	-
Sb	< 6	< 6	< 6	< 6	< 6	< 6	< 6	-
Pb	7	6	8	6	12	6-12	10	-
B	0.6	0.2	0.4	0.7	< 0.2	< 0.2	0.2-0.6	0.3
Si	600	600	600	240	60-70	60-70	95	70
V	< 4	< 4	< 4	< 4	< 30	< 30	< 30	< 10
Co	< 7	< 7	< 7	< 7	-	-	-	< 2
Sr	< 6	< 50	< 50	< 50	< 50	< 50	< 25	-
Ag	< 1	< 1	< 1	< 1	< 1	< 1	< 1	-
Ba	< 6	< 6	< 6	< 6	< 6	< 6	< 6	-
Bi	< 2	< 2	< 2	< 2	< 2	< 2	< 2	-
Na	5	2	5	1	1-2	1-4	< 1	< 1
P	< 120	< 120	< 120	< 120	< 120	3	< 120	-
Cr	2	2	2	10	5-9	2-6	1	8
Ni	12	12	12	30	12	6-12	6	32
Zr	< 35	< 35	< 35	< 12	-	-	-	-
Cd	< 2	< 2	< 2	< 2	< 2	< 2	< 2	-
Ta	< 50	< 60	< 60	< 60	-	-	-	-

TABLE III

COMPARISON OF PRELIMINARY CHARACTERIZATION OF SEVERAL LOTS OF URANIUM

CARBON AND HYDROGEN ANALYSIS

<u>Material</u>	<u>Carbon</u>	<u>Hydrogen</u>	<u>Grain Size ASTM No.</u>	<u>Hardness DPH</u>
U, CM-3-8400	< 100	0.19	9	213
U, 69072-39	290	0.8	7-8	265
U, CMB-6-70234	~ 300	0.4	1-3	243
U, LASL-2233	120	0.17	8	
U, CMB-6-C1-900	95	*		
U, CMB-6-C1-901	68	*		
U, CMB-6-C1-903	142	*		

* Analysis pending

The sheet specimens were 0.76-mm thick and had a gage section 12.7-mm long; the round specimens were 2.3-mm diam and had a gage section 25.4-mm long.

Results from three specimens tested near the upper temperature limit of the alpha phase and two tested in the lower temperature region of the gamma phase are shown in Table IV. The specimens tested in the high alpha region showed excellent ductility, about 75% elongation and 68% reduction in area. Photographs of both the sheet and round specimens after tensile testing are shown in Fig. 3. The alpha phase exhibits substantial strain hardening at these elevated temperatures as indicated by the large amount of relatively uniform stretching of the gage sections. This is consistent with the stress-strain curves for the alpha phase shown in Fig. 1.

The plastic anisotropy factor, R, was estimated from measurements on the deformed cross sections as 3.7 which yields a Z/X (strength in thickness direction to strength in the plane directions ratio) of 1.5. The alpha phase retains much of its room temperature anisotropic character at elevated temperatures, ~ 550°C, when tested at high strain rates, ~ 3000 s⁻¹.

The deformation at 800°C, in the lower gamma region, was much more localized as shown in Fig. 4. The total elongations for the sheet and round specimens were only 15 and 25% respectively, yet the reductions in area were ~ 99% with the specimens necking down to a chisel point in the sheet and a pin point in the round specimen. Local axial strain measurements in the round specimen showed strain levels of only 10% near the button heads but strains were as high as ~ 350% in the necked region. An estimate of the R-value made from the low strain region was 1.4;

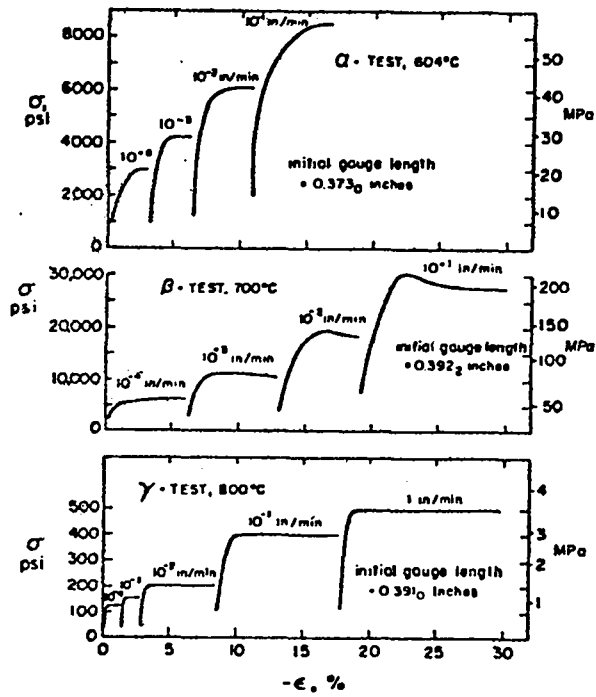
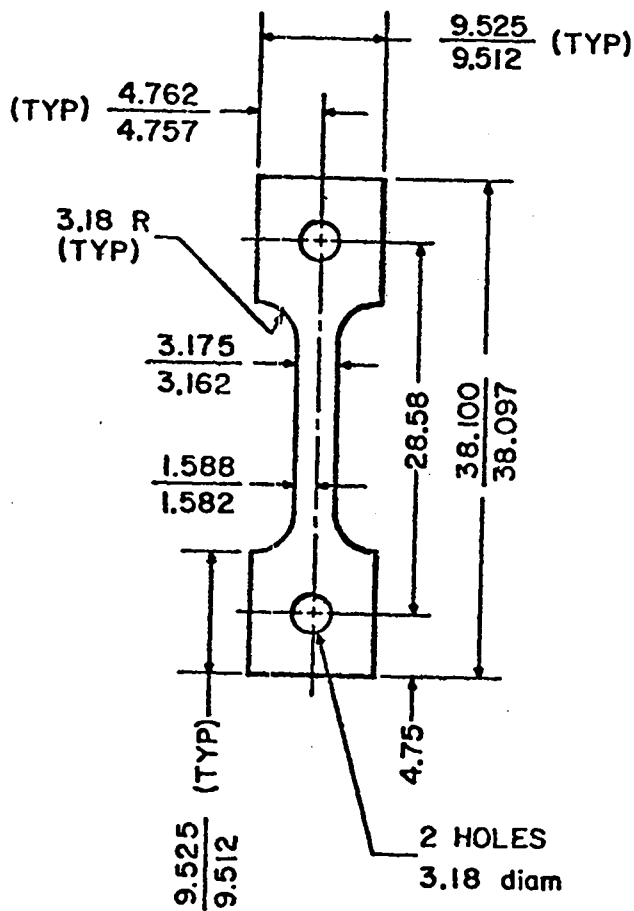


Fig. 1. Low strain rate true stress-true strain curves for compression tested α , β , and γ uranium, LA 2233 material. From reference 2



A tensile test specimen. Dimensions are in millimeters.

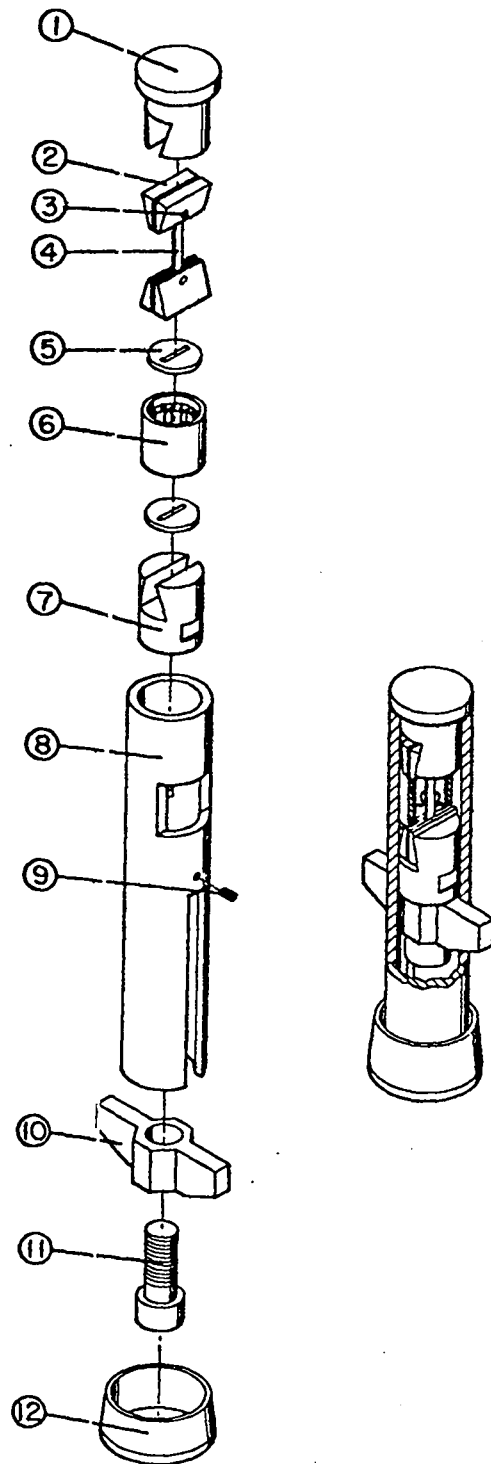
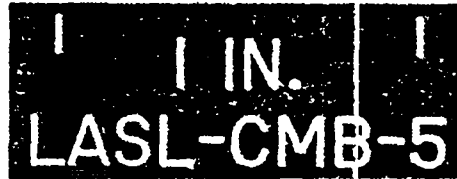
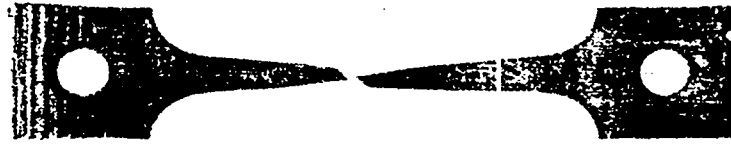


Fig. 2. Fixtures, specimen, and furnace for high-rate tensile tests. (1) Top grip, (2) Wedges, (3) Guide pin, (4) Specimen, (5) Radiation shield, (6) Furnace, (7) Bottom grip, (8) Tubular support, (9) Setscrew used for assembly, (10) Driver bar, (11) Loading screw, and (12) Deformable copper ring.
From reference 2.

TABLE IV

TENSILE TESTS AT HIGH TEMPERATURES AND ON CM 3 8480 MATERIAL

<u>SPECIMEN</u>	<u>TYPE OF SPECIMEN</u>	<u>TEST TEMPERATURE °C</u>	<u>STRAIN RATE $\frac{1}{s}$</u>	<u>TOTAL ELONGATION %</u>	<u>REDUCTION IN AREA (%)</u>	<u>R-VALUE</u>	<u>Z/X</u>
PA2-141-7T	Sheet	535	~3000	84	69	-	-
PA2-141-5P	Sheet	550	~3000	74	63	-	-
PA2-141-6P	Sheet	800	~3000	15	99	-	-
PA2-137-19A	Round	550	~3000	66	71	3.7	1.5
PA-2-141-9B	Round	800	~3000	26	99	1.4	1.1



Sheet Specimen



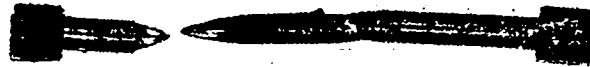
Round specimen

Fig. 3. Fractured CM 3 8480 tensile specimen tested at 550°C and a projectile velocity of 45 ms⁻¹.



1 IN.
LASL-CMB-5

Sheet specimen



1 IN.
LASL-CMB-5

Round specimen

Fig. 4. Fractured CM 3 8480 tensile specimens tested at 800°C and projectile velocity of 45 ms⁻¹.

$Z/X = 1.1$. Apparently transformation to the bcc gamma phase destroyed the strong texture present in the orthorhombic alpha phase. The relatively small total elongations combined with the very high local ductility indicated a lack of strain hardening and a large strain rate sensitivity which provides for a large local ductility. This is in agreement with the results shown in Fig. 1 for compression tests a specially prepared isotropic uranium, LA 2233.

The elevated temperature-high strain rate specimens tested in the alpha region at 550°C failed in the center of the gage section where the highest temperature existed as shown in Fig. 3. A peculiar failure geometry was apparent in both sheet and round samples tested in the gamma region at 800°C as shown in Fig. 4. Failure occurred near one end of the gage length by localized necking. The necked region of the specimen consisted of most of the gage section and showed a normal smoothly tapering profile; however, the grip section showed an abrupt transition from the cylindrical section to a tapered profile. The deformed region near the center of the round specimen was caused by interaction with furnace parts after the initial failure.

The sharp demarcation line on the left grip section of the necked portions at each specimen is quite evident in Fig. 4. Figure 5 shows SEM photographs of the necked region including the fracture surface (lower picture) and final fracture surface at a much higher magnification (upper picture) of the sheet specimen. The final fracture occurred only after necking to a sharp chisel-like point. Figure 6 shows SEM photographs of two views of the necked region near the grip end of the round tensile specimen; the same general behavior took place. The pattern evident on the necked region in the foreground of the top picture in Fig. 6 was caused by surface oxide on the specimen cracking as the surface stretched. The final fracture surface of this specimen is pictured in Fig. 7. The uranium has obviously undergone extreme deformation before fracturing.

The probable explanation for the unusual, (i.e., the sharp demarcation between the deformed and undeformed regions) behavior of the specimens tested at 800° involves the temperature gradients imposed by the specimen heater. The heater fitted closely around the specimen gage section but only indirectly heated the grips leading to a temperature gradient between the gage and grip section. The line of demarcation between deformed and undeformed material was likely at the beta to gamma phase transition in uranium. Since the beta phase is much stronger it would resist deformation, while the more ductile and weaker gamma phase would readily deform. A stress concentration caused by the higher stiffness of beta relative to gamma would be expected at the beta-to-gamma interface. This would result in a higher local stress at the interface than at the center of the gage length and yielding could start there in spite of the higher temperature expected at the center of the gage length.

3.2 Biaxial Test

Two biaxial tests were performed in the alpha region at 550°C at a projectile velocity of 45 ms⁻¹ producing a strain rate of about 2000 s⁻¹.



Final fracture surface

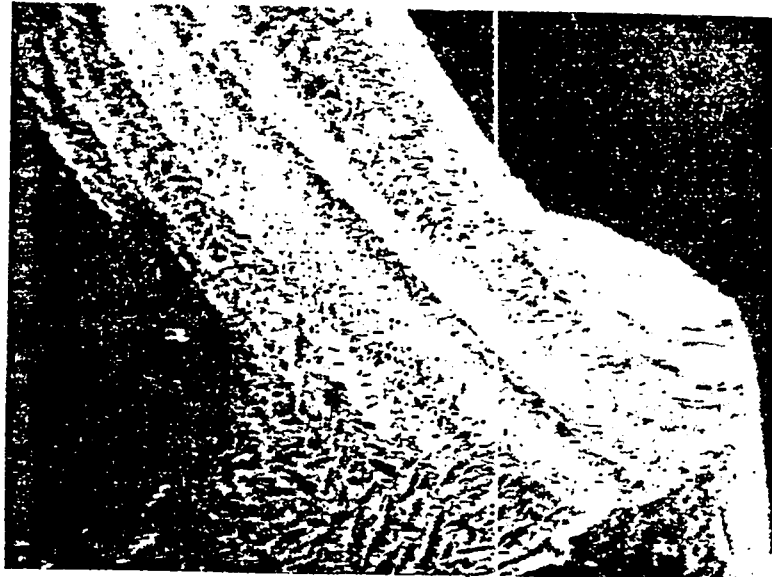
2500X



Fracture and necked surface

50X

Fig. 5. SEM photographs of grip-end fracture surface of sheet tensile specimen of CM 3 8480, tested at 800°C with a projectile velocity of 45 ms⁻¹.



75X



25X

Fig. 6. SEM photographs of the fracture surface of the grip-end of a CM 3 8480 round tensile specimen tested at 800°C with a projectile velocity of 45 ms⁻¹.



250X

Fig. 7. SEM photograph of fracture surface of grip end of a CM 3 8480 round tensile specimen tested at 800°C with a projectile velocity of 45 ms⁻¹.

The hold-down grooves were formed at 200°C before testing. A MoS₂ lubricated punch was employed. Tensile strains at fracture were certainly biaxial in nature falling between the condition of plane strain and balanced biaxial strain. Maximum uniform strains of 22% and 30% were measured in the two samples. These values are much lower than the total elongations of ~ 70% measured in uniaxial tension. The stress state appears to have a strong effect on ductility of this uranium.

4. 69072 URANIUM, RUN-OF-THE-MILL URANIUM

The history insofar as it could be determined of this material, which consists of many sheets of a lot of uranium made at the Oak Ridge Y-12 plant, was discussed in the last quarterly report¹. Mechanical property data are being accumulated on a particular sheet, 69072-39, of this lot of uranium and may differ somewhat from other sheets; however, it was selected to have the same chemistry as the sheets used for liner tests. Some differences between sheets must be expected and are typical of production grade uranium.

This material has been characterized at room temperature using round specimen tensile tests in two perpendicular directions in the plane of the sheet and by compression tests in these directions and in the through thickness direction. The round tensile specimens were 2.29-mm diam with a 12.7-mm-long gage section. Compression specimens in the plane directions were 3.2-mm diam by 10.2-mm-long while those in the through thickness direction was 2.29-mm diam by 3.56-mm long. The data generated at a strain rate of $6.7 \times 10^{-4} \text{ s}^{-1}$ is shown in Table V. High strain rate tensile tests are now underway. Electropolishing the samples to remove surface defects increased the ductilities substantially. The parallel direction is considerably stronger than the transverse direction. This is shown in Fig. 8 which compares the tensile stress strain behavior of the 69072-39 and CM 3 8480 (dashed lines) material.

The 69072-39 uranium is considerably stronger, but less ductile and shows slightly more in-plane anisotropic behavior than the CM 3 8480 material in its tensile behavior.

The compression test results, shown in Fig. 9 are similar to the tensile results. There is a moderate strength anisotropy in the plane and a strong anisotropy between the thickness and plane directions with the thickness direction much stronger. The inflection in the transverse direction compression stress strain curve is similar to that observed to both the CM 3 8480 and 69072-39 transverse tensile stress strain curves.

5. CAST URANIUM, CMB-6-70234

The material examined was one of three identical castings made from the same feed stock. Two were used in liner tests and one cut up for characterization. Processing history of these materials was discussed last quarter.

TABLE V

ROOM TEMPERATURE TENSILE TEST RESULTS OF LASL 69072-39
UNALLOYED URANIUM SHEET, STRAIN RATE $6.7 \times 10^{-4} \text{ s}^{-1}$

SAMPLE	CONDITION	TOTAL	ULTIMATE TENSILE	REDUCTION	R	Z/X
		ELONGATION	STRESS	IN AREA		
		%	MPa (ksi)	%		
1	As rec'd, T ^(a)	20	-	17.5	-	-
2	As rec'd, T	21	-	13.7	-	-
3	Electropolished, T	35.5	900 (131)	33.1	6.4	1.9
4	Electropolished, T	35.3	890 (130)	36.8	6.8	2.0
5	Electropolished, P	-	-	30.9	2.9	1.4
6	Electropolished, P	25	980 (142)	31.0	3.7	1.5
7	Electropolished, P	29	970 (140)	-	-	-

(a) T = Transverse direction from rolling direction.
P = Parallel direction to rolling direction.

Round tensile specimens were obtained from three locations in the hemispherical casting number CMB-6-70234. Location one was close to the pole with the sample axis parallel to a meridian, location two was close to the equator with the sample axis parallel to a meridian and location three was close to the equator with the sample axis parallel to the equator. The specimens had a 2.29-mm-diam and a 12.7-mm-long gage length.

There was a wide variation in properties of this material in part because of its very large grain size; some grains extended completely through the gage section. The ductilities of the specimens were much less in this cast material than for the wrought materials. While all the specimens showed some ductility, their strain histories, Fig. 10, indicated that the normal necking process was pre-empted by another mechanism causing failure.

It is clear that normal as-cast uranium would be an inferior liner material.

6. URANIUM CMB-6-C1-900

This material is a low carbon unalloyed uranium which was cast and subsequently extruded into a 50-mm-diam rod¹. The feed stock had a carbon content of 45 to 80 ppm which increased to 90 to 100 ppm upon casting. The 50-mm-diam extrusions were then high energy rate (HER) forged at 450°C to a reduction in height of ~ 58%.

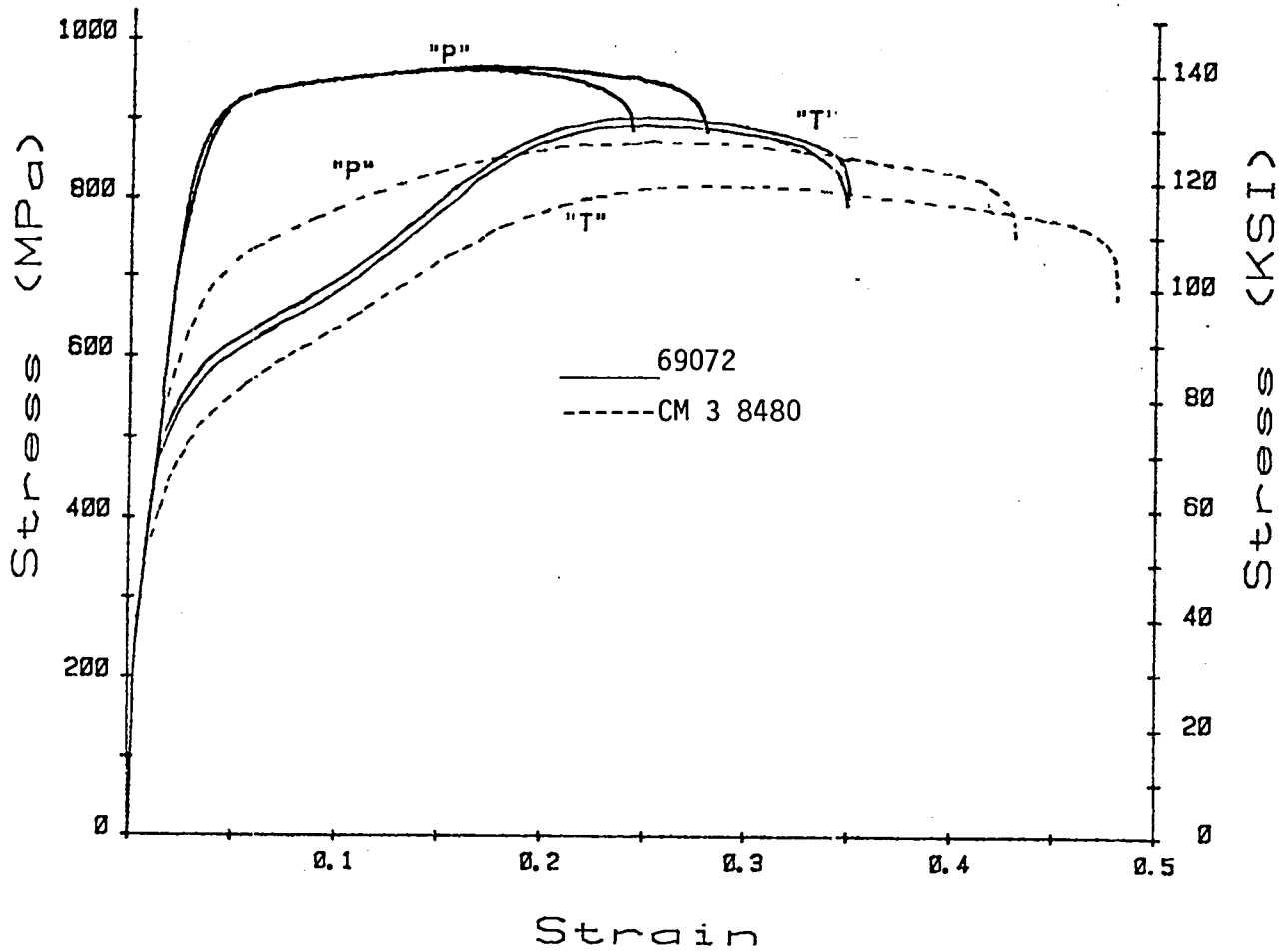


Fig. 8. Tensile test results for 69072-39 and CM 3 8480 uranium at room temperature and a strain rate of $6.7 \times 10^{-4} \text{ s}^{-1}$. "P" and "T" samples were taken at mutually perpendicular sheet directions.

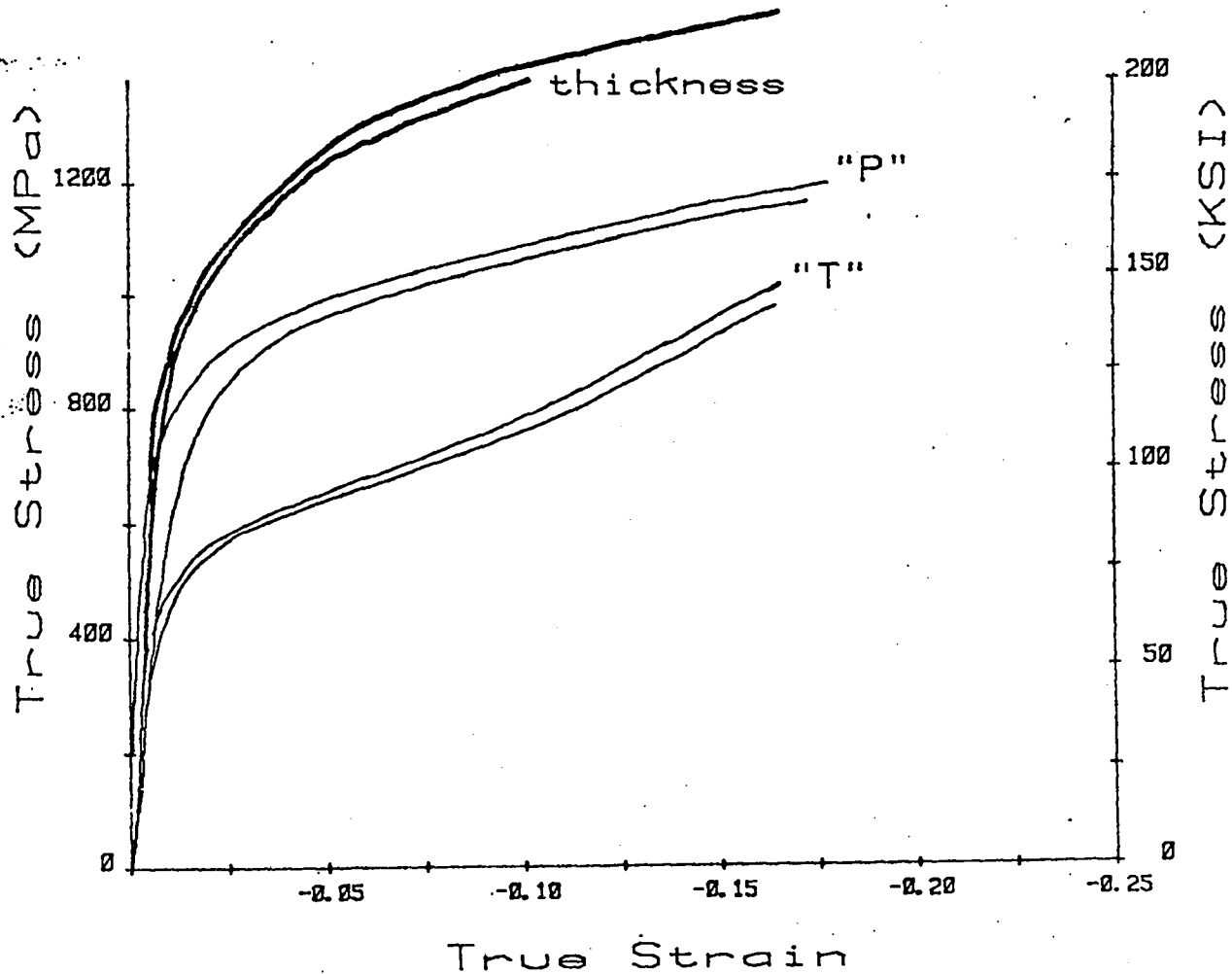


Fig. 9. Compression test results on samples from sheet 69072-39. Tests were conducted at room temperature at strain rates of about 10^{-4} s^{-1} . "P" and "T" samples were taken with their axes in mutually perpendicular direction within the plane of the sheet.

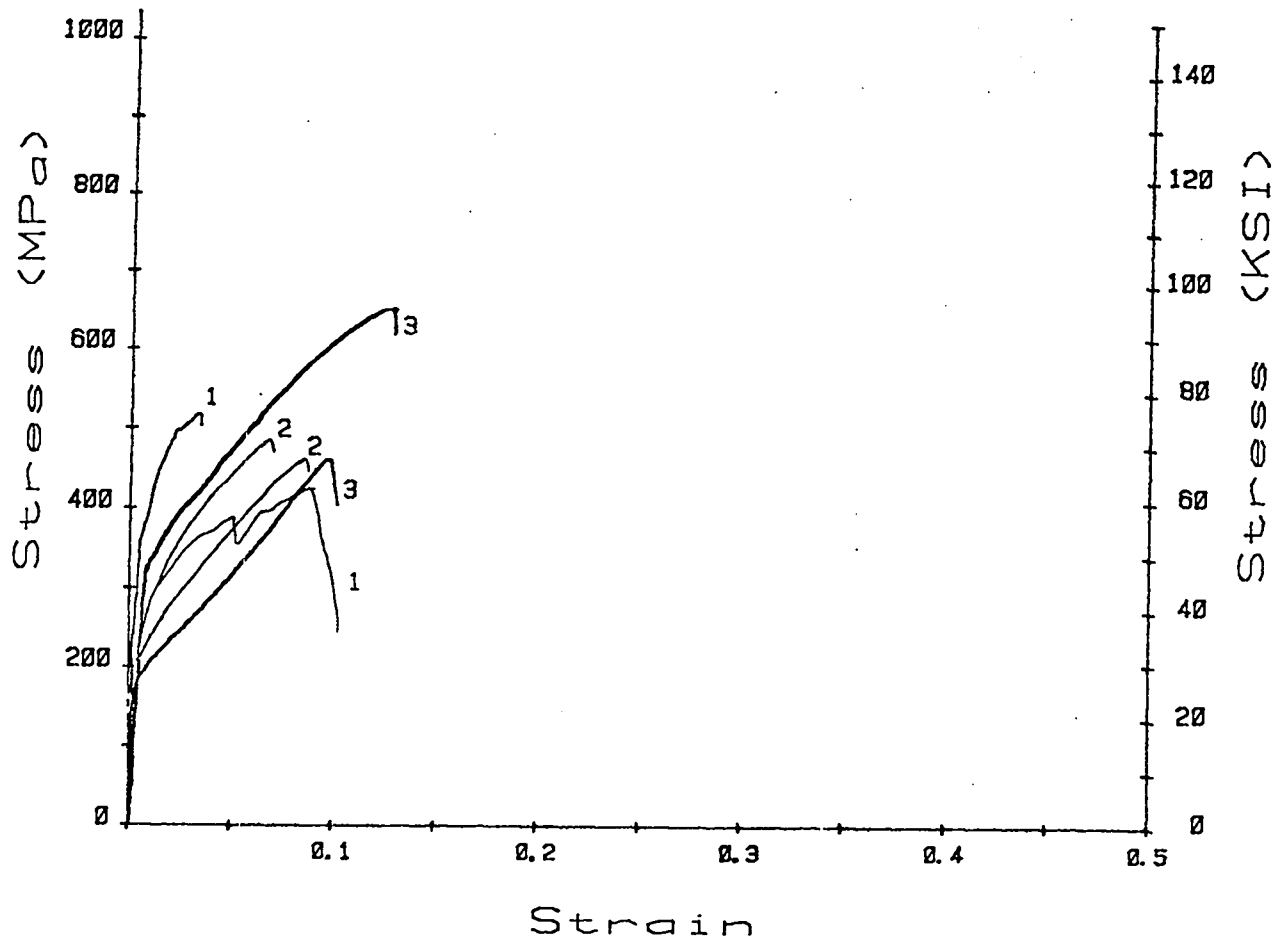


Fig. 10. Room temperature tensile test results on LASL CMB-6-70234 hemishell casting at a strain rate of $6.7 \times 10^{-4} \text{ s}^{-1}$. Samples labeled "1" were taken on a meridian close to the pole. Samples labeled "2" were taken on a meridian close to the equator. Samples labeled "3" were taken at the equator in an equatorial direction.

At this point we determined the final processing conditions desirable to impart a reasonably uniform and fine recrystallized grain size to this material. One of the as-forged billets was re-struck (HER forged) at 450°C to a final height of 10.4 mm. A second identical billet was warm rolled at 325°C ~ 80% to a final thickness of 3.7 mm. Samples from each of these sheets were vacuum annealed at 625°C for 1 h along with a sample from one of the original forgings. All samples were subsequently examined metallographically (Figs. 11 and 12). It is obvious from these microstructures, that the material which had been warm rolled, displayed the most uniform and smallest grain size of the three samples. Therefore, the remaining forgings were similarly warm rolled and annealed. Since the microstructure of these appeared to be very uniform, several of the warm rolled and annealed pieces were machined into circular blanks and these were deep drawn into hemishells in an identical fashion to those used for previous liner test related to this program.

The drawn shells were vacuum stress relieved at 400°C for 30 min after forming. One of these has been machined into a finished liner. A second was examined metallographically which confirmed that the structure was uniform and fine-grained throughout. Fig. 13 shows the excellent microstructure of this shell. The average hardness of the shell was DPH 226 (hardness range of DPH 210-245). The liner machined from this lot of unalloyed uranium, CMB-6-C1-900, will be the first to be fired for which a complete processing history is available.

Sufficient sheet stock of this material for a complete characterization at both high and normal strain rates has been prepared and sample machining is well underway. Testing is expected to get underway shortly.

6. URANIUM CMB-6-C1-901

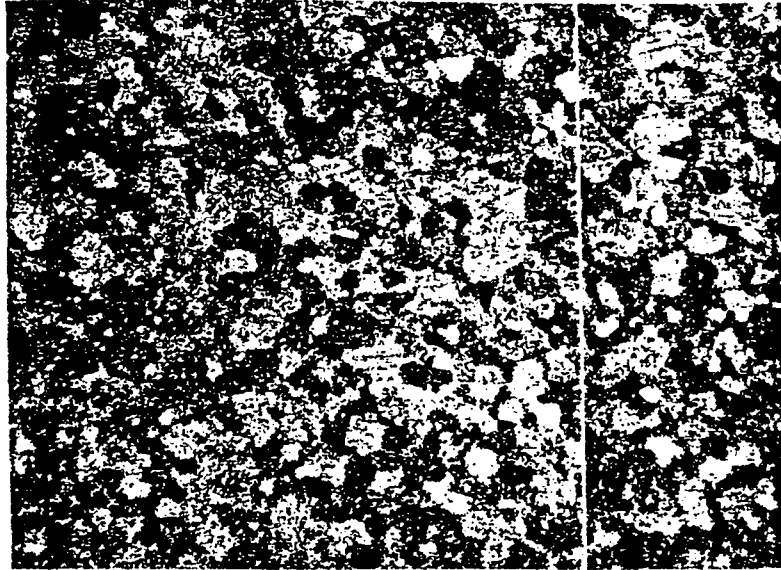
The material was fabricated in a very similar manner to CMB-6-C1-900. The fabrication history was included in last quarter report. A different feed stock containing ~ 20 ppm carbon was used which resulted in a billet containing 68 ppm carbon. The fabrication of this material has been completed and it also is being machined into test specimens. Material has been reserved to make liners for testing purposes, if so desired.

7. URANIUM CMB-6-C1-903

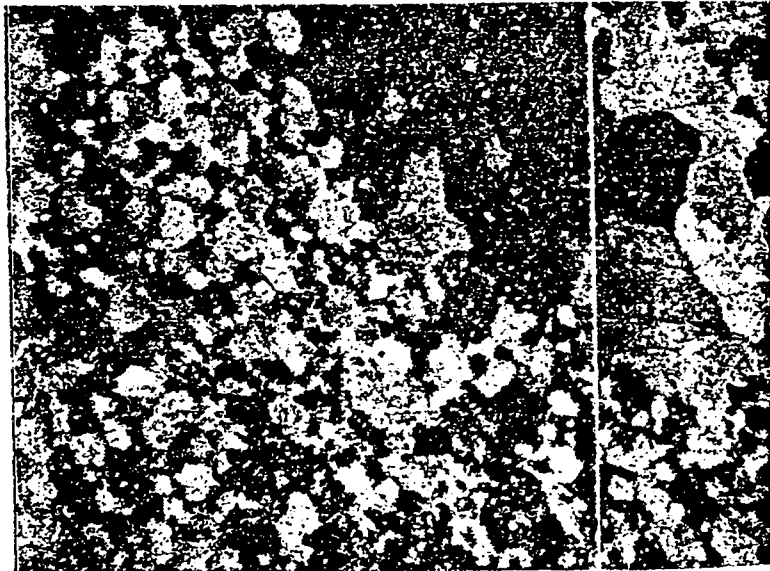
This material is an "extra" made in the form of a plate casting using the same feed stock as was used for CMB-6-C1-900 which was cast as a rod. It is being processed using only a combination of hot and warm rolling - no extrusion or forging - to compare properties of identical material fabricated in two different ways with completely known histories.

8. HOPKINSON SPLIT PRESSURE BAR TESTING PROGRAM

Our Hopkinson bar has been installed and is undergoing its first real tests. Several room temperature experiments have been conducted to verify the operation. Cabra 360 brass in the half-hard condition and 316 stainless steel were chosen for the first tests. The stainless steel

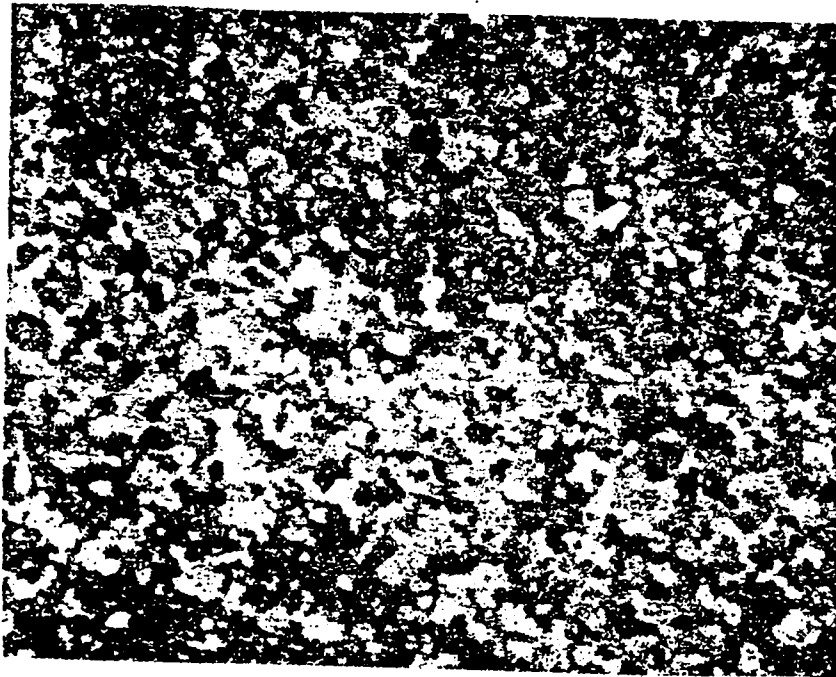


Extruded (850°C), forged (450°C) and annealed (625°C/1 h/vacuum). Grain size: ASTM 5-7.
100X



Extruded (850°C), double forged (450°C) and annealed (625°C/1 h/vacuum). Duplex grain size: ASTM 3, 7.
100X

Fig. 11. Processed unalloyed uranium CMB-6-C1-900.



100X

Fig. 12. Processed unalloyed uranium, CMB-6-C1-900; extruded (850°C), forged (450°C), rolled (325°C), and annealed (625°C/1 h/vacuum). Grain size ASTM 7-1/2.



100X

Fig. 13. Typical microstructure of drawn and stress-relieved (400°C/30 min/vacuum) unalloyed uranium hemispherical shell from LASL CMB-6-C1-900. Material had been extruded, forged, warm-rolled, and annealed prior to forming of shell. Grain size ASTM 8.

will be used when the higher yield strength incident and transmitter bars are installed. Brass specimens were 7.62- and 8.38-mm diam with length-to-diam ratios of 1-4, 1-5, and 2-5

Fig. 14 shows the results from a series of representative tests on brass specimens; the agreement between tests seems to be adequate. A computer program has been written to process the Hopkinson bar data and average results from the Hopkinson bar tests are compared with low strain rate compression tests in Fig. 15. The results indicate a strain rate sensitivity and possibly an increased strain hardening at the higher strain rate for the brass.

Following these tests high strength bars of Vasco Max 350 maraging steel were installed. After these preliminary tests with 316 stainless steels the first uranium specimens will be tested.

To increase the usefulness of the Hopkinson bar a furnace is being designed and will be installed on the apparatus to provide a high temperature capability.

9. DISCUSSION

9.1 Low Strain Rate Test Results

A considerable amount of room temperature characterization and some high temperature characterization have been completed on four uranium materials, CM 3 8480, 69072-39, CMB-6-70324 and LA 2233. In addition, uranium CMB-6-C1-900 and CMB-6-C1-901 have been prepared and are in the sample preparation stage, while CMB-6-C1-903 has been cast.

Liners have been prepared from CM 3 8480, 69072-39, cast material identical to 70324 and CMB-6-C1-900; all have been fired except CMB-6-C1-900. There were significant differences in the performance of the liners and we have found differences in the materials that help explain the liner results. Liner tests have indicated that CM 3 8480 is the best of the three tested materials, 69072 is intermediate and the cast material from the 70324 series is the poorest.

Photomicrographs in the last quarterly report¹ showed the very large, ASTM 1 to 3, grain size of the cast material. Indeed, some tensile samples and, therefore, the liners had residual gamma grains extending completely across the cross section. Fig. 16 contains two SEM views of the fracture surface of the cast material showing mixed mode fracture patterns. Intragranular cleavage areas are linked by regions of ductile dimple fracture. Apparently intragranular cleavage after about 10% ductile strain terminated all the tensile test on the cast materials. We would not expect such a material to perform well as liners, and it didn't.

Uranium 69072 is a much finer grained uranium rather typical of production grade uranium. This type of uranium tends to fracture by a ductile failure mode, which is thought to occur by linking of cracks propagating from nucleation sites, which can be inclusions. Uranium is particularly susceptible to this type of failure, since it contains many

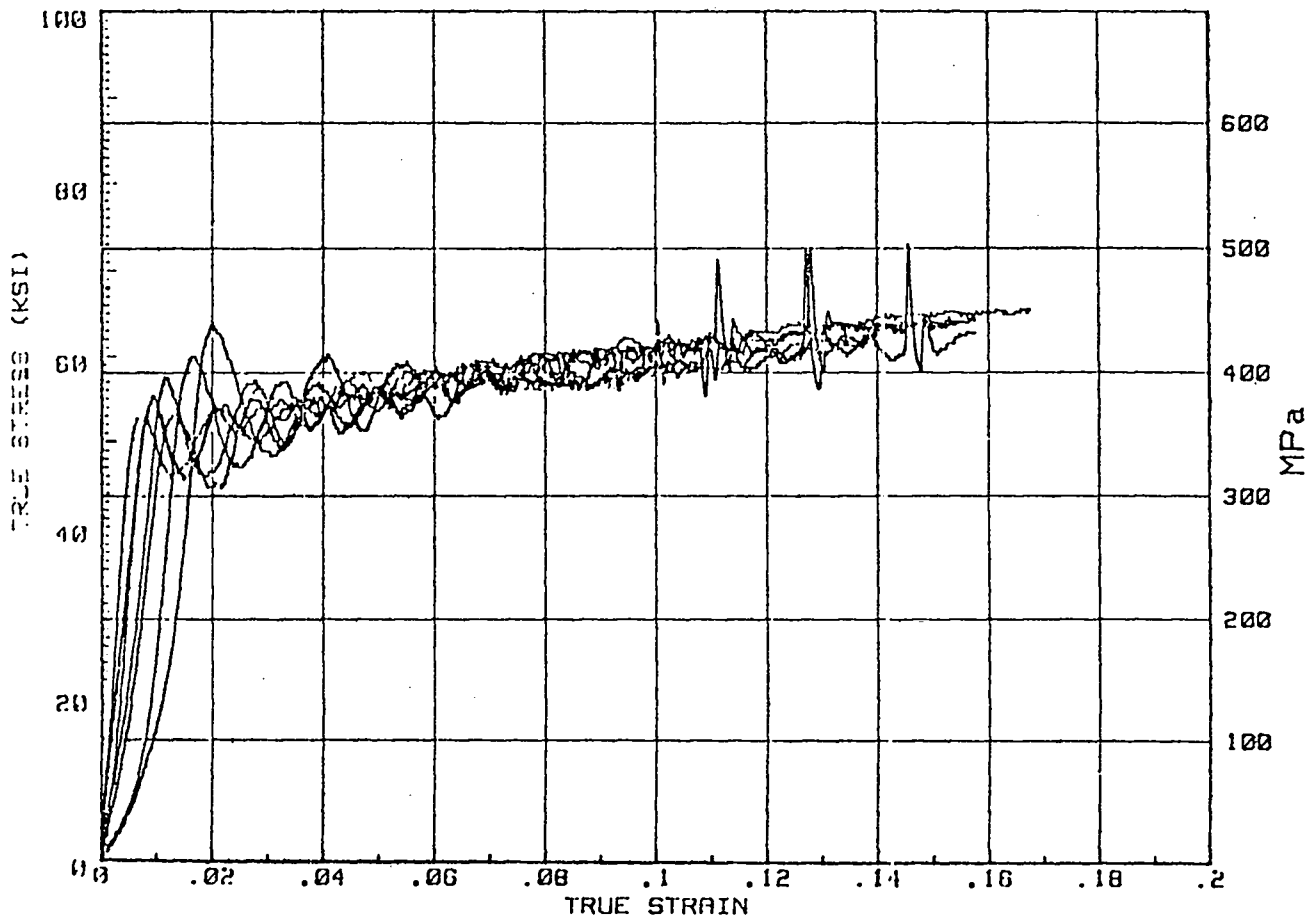


Fig. 14. Hopkinson Bar Compression Data from representative tests of Cabra 360 half-hard brass samples obtained at a test temperature of 25°C and $2 \times 10^3 \text{ s}^{-1}$ strain rate.

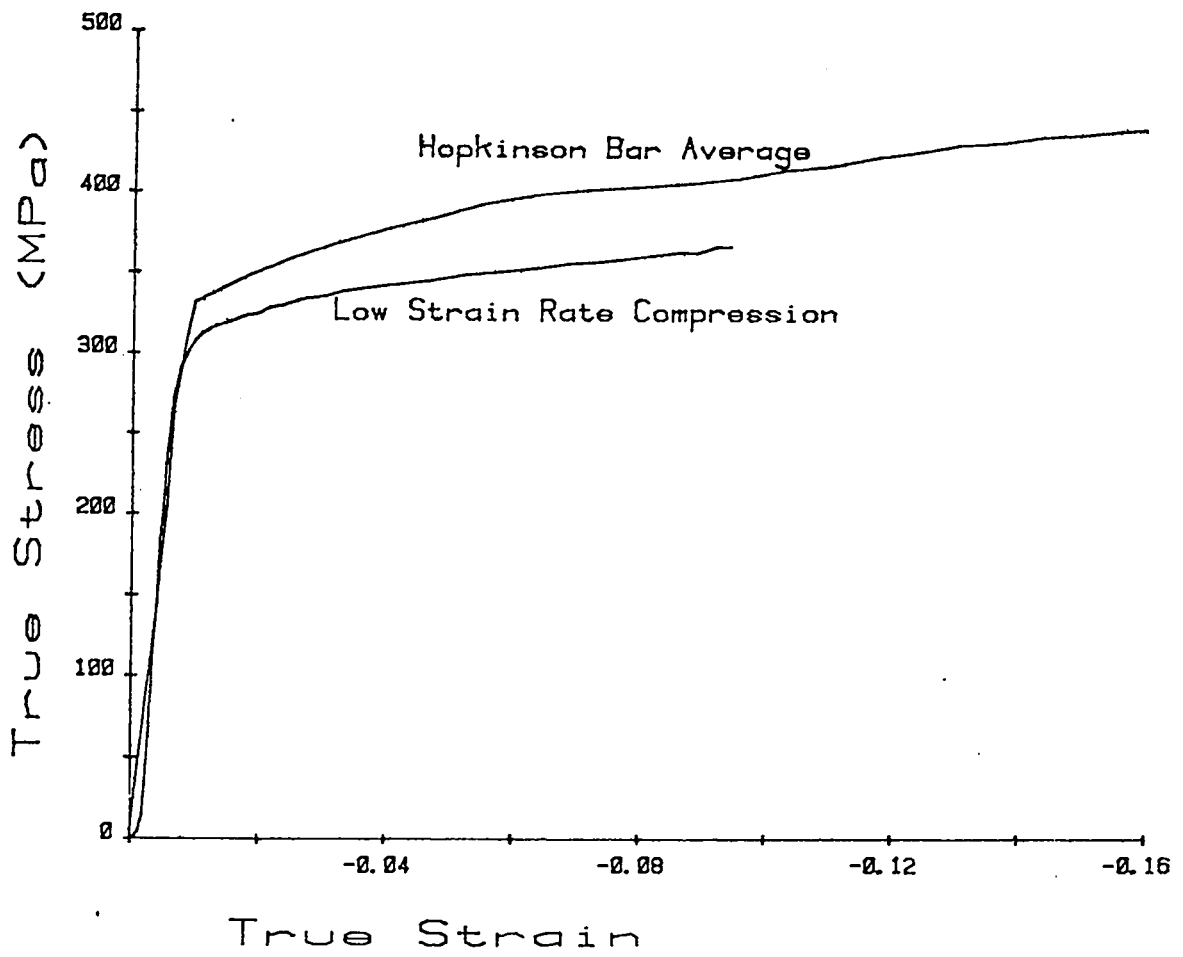
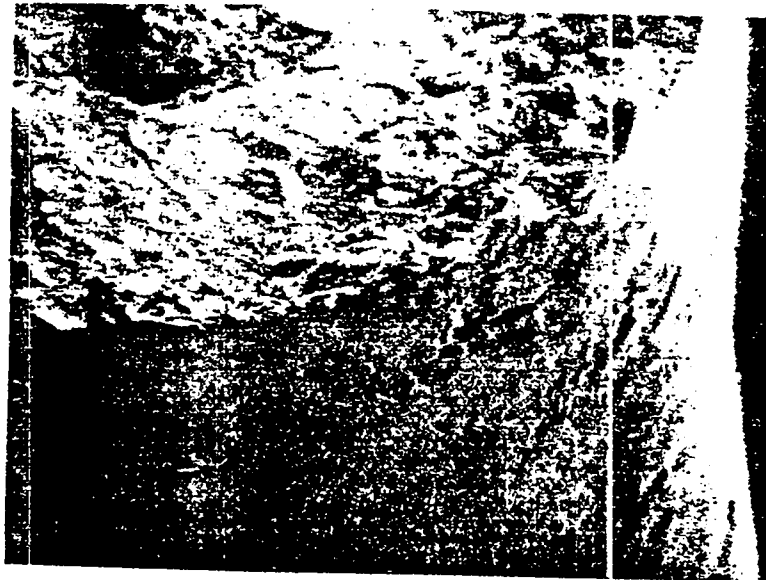


Fig. 15. Comparison of compression tests on Cabra 360 half-hard brass. Hopkinson Bar Average Data at a strain rate of $2 \times 10^3 \text{ s}^{-1}$. Instron Test Machine data at a strain rate of $6 \times 10^{-4} \text{ s}^{-1}$.



60X



60X

Fig. 16. SEM photographs of round tensile specimen of LASL casting CMB-6-70234 after testing. Bottom fracture surface shows intragranular cleavage. Top: Cylindrical surface showing circumferential cracks.

inclusions, mostly carbides. It is difficult to keep the carbon content of production grade uranium low enough to prevent the formation of relatively large concentrations of the insoluble uranium carbide. Fig. 17 shows a typical carbide particle (upper photograph) in the grip section of a 69072 sample where little or no plastic deformation has occurred, and a similar shattered particle near the fracture surface which has begun to propagate a crack (lower photograph).

The carbon content of the 69072 material is ~ 290 ppm compared to ~ 300 for the cast material, 70324, and less than 100 for the CM 3 8480 material. The relative concentrations of inclusions in these three materials can be judged from the metallographic cross sections of tensile specimens shown in Fig. 18. The center photograph of the run-of-the mill uranium, 69072, has both more and larger inclusions than the CM 3 8480 material (bottom) while the cast, 70324, material (top) is intermediate. The cast material fractured at a much lower strain than the other two materials, and its inclusions have not debonded as severely.

Numerous surface cracks are visible near the fracture surface of the 69072 material as shown in the bottom photomicrograph of Fig. 19. The fracture surface of the material is shown in the top picture and has a uniform ductile fracture appearance. The crack morphology is clearer when examined at a higher magnification as shown in Fig. 20. The surface cracks are pictured in the bottom photomicrograph and cracks propagating from an inclusion on the fracture surface in the top picture.

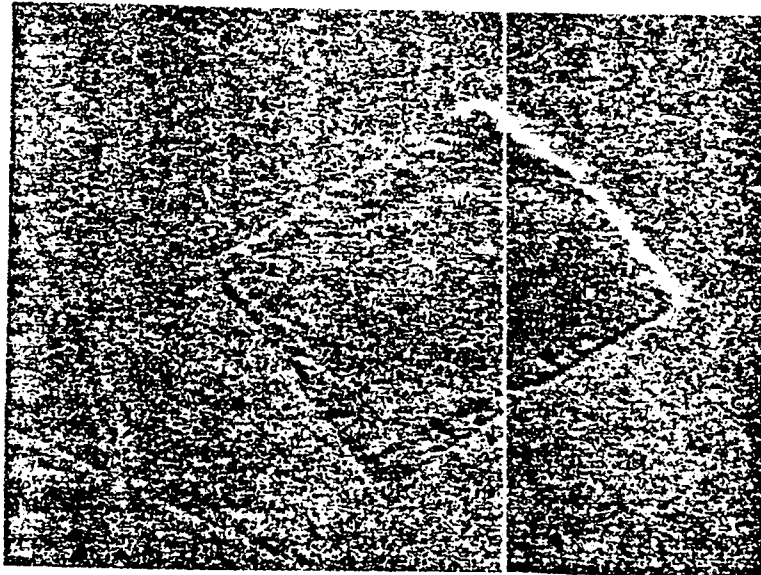
The cylindrical surface and fracture surface of the CM 3 8480 material are shown in SEM photographs on Fig. 21. The fracture surface shown on the top picture had several large facets at roughly 45° to the specimen axis with a relatively fine ductile fracture pattern over all. There were relatively few circumferential cracks in this material.

The data certainly implies a relationship between inclusion content and ductility of uranium at room temperature and a slow strain rate. Future tests will allow an evaluation of similar properties as a function of strain rates and temperature. High strain rate data for the CM 3 8480 have been obtained and are presently being obtained on the 69072 material.

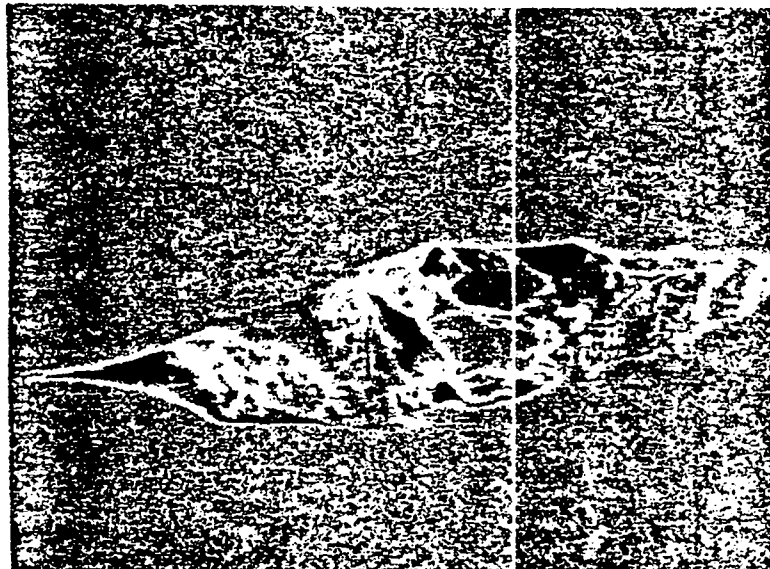
9.2 High Temperature-High Strain Rate Results

The high temperature-high strain rate results are quite interesting and there is at least a good qualitative correlation between the published results of Taplin⁴ and Loretan and Murphy⁵ (shown in Fig. 22) at slow strain rates and our results at high strain rates. All of these test results indicate a sharp discontinuous drop in strength going from beta to gamma phase at high strain rates. At high strain rates the alpha phase retains good strain hardening as well as excellent elongation at 550°C .

The gamma phase, on the other hand, has little capacity for strain hardening and deforms almost entirely by localized necking. We have yet to measure ductility in the beta phase region but would expect it to be low. These measurements are underway.



5000X



2500X

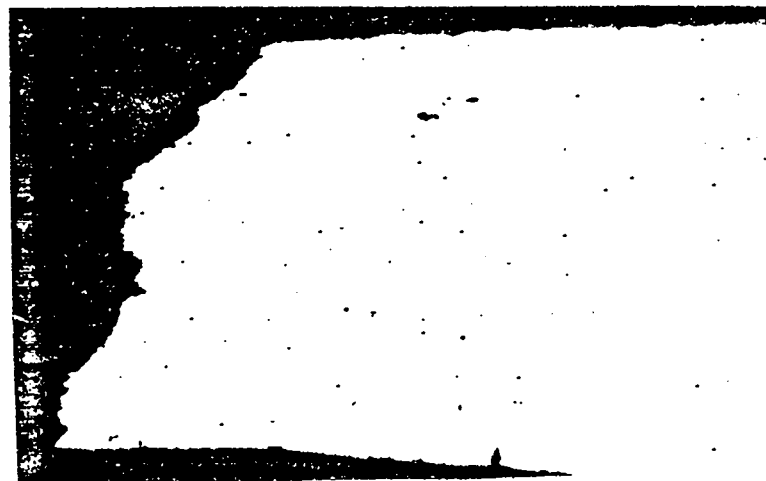
Fig. 17. Carbide inclusions in unstrained grip section of 69072-39 round tensile specimen. Tensile axis horizontal in pictures. Top: Unbroken inclusion well-bonded to matrix. Bottom: Broken carbide inclusion near fracture surface



Cast uranium, CMB-6-70324

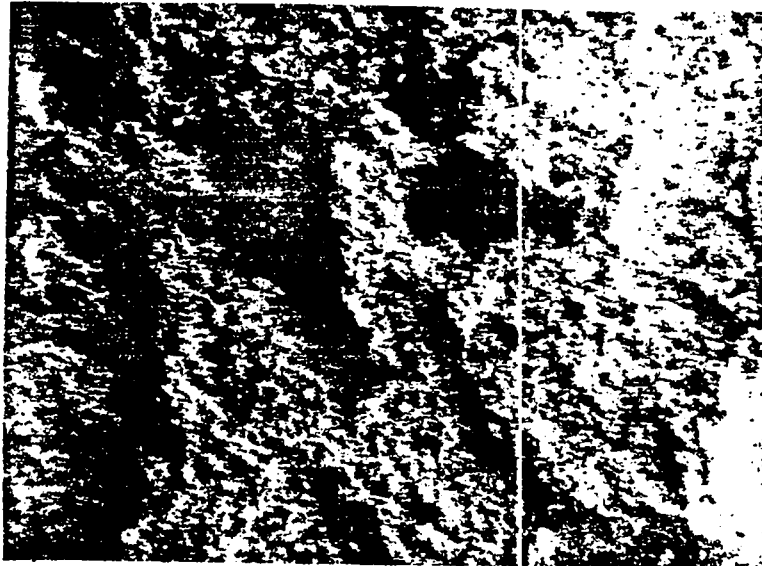


Run-of-the-mill uranium 60972-39

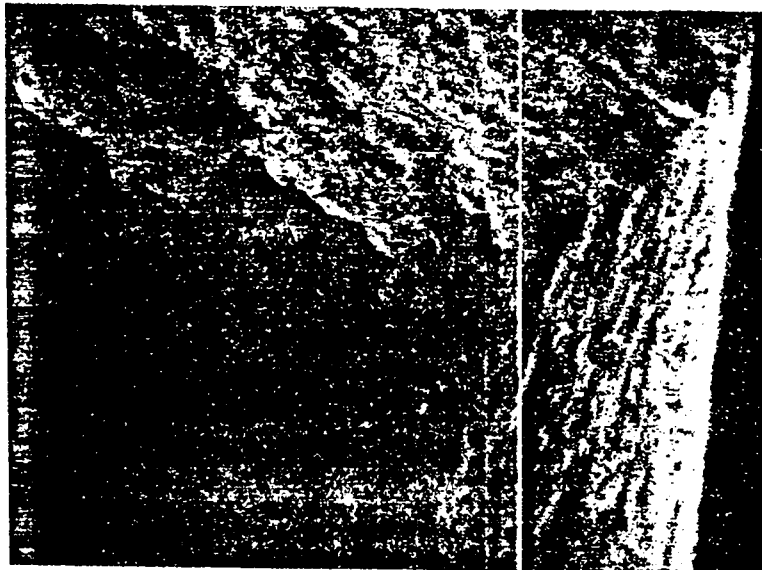


Special uranium CM 3 8480

Fig. 18. Longitudinal metallographic section near fracture of 2.29-mm-diam tensile specimens tested at $6.7 \times 10^{-4} \text{ s}^{-1}$.



75X



75X

Fig. 19. SEM photographs of round tensile specimens of 69072-39 tested at 25°C at a strain rate of $6.7 \times 10^{-4} \text{ s}^{-1}$. "P" direction. Top: Fracture surface. Bottom: Cylindrical surface showing circumferential cracks.

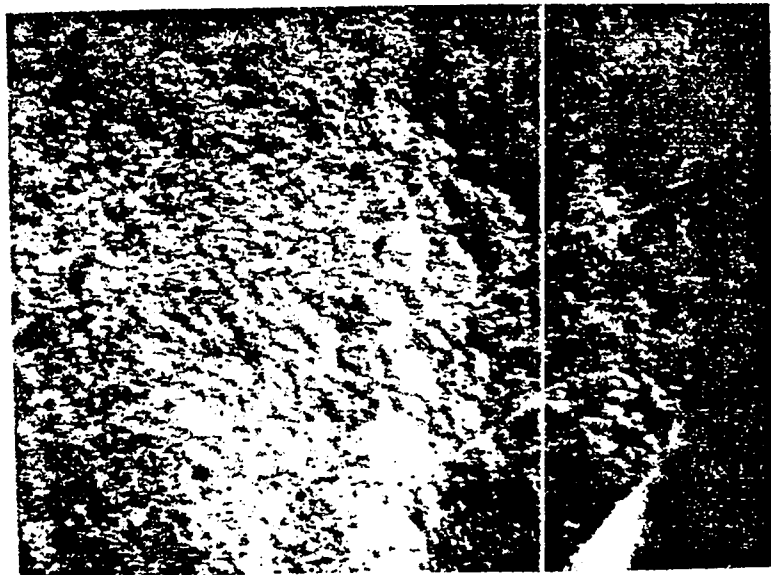


2000X

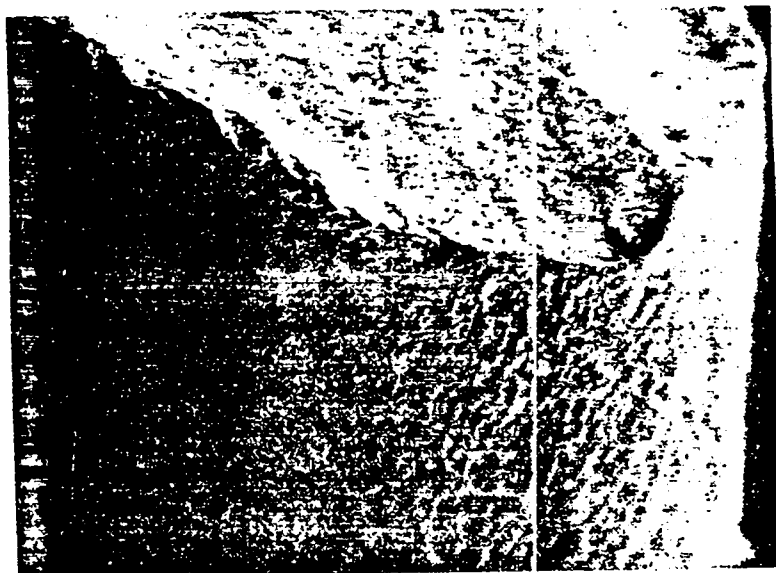


500X

Fig. 20. SEM photographs of 69072-39 round tensile specimen after testing at 25°C at a strain rate of $6.7 \times 10^{-4} \text{ s}^{-1}$. Top: Crack propagated from carbide particle in fracture surface. Bottom: Circumferential cracks in cylindrical surface.

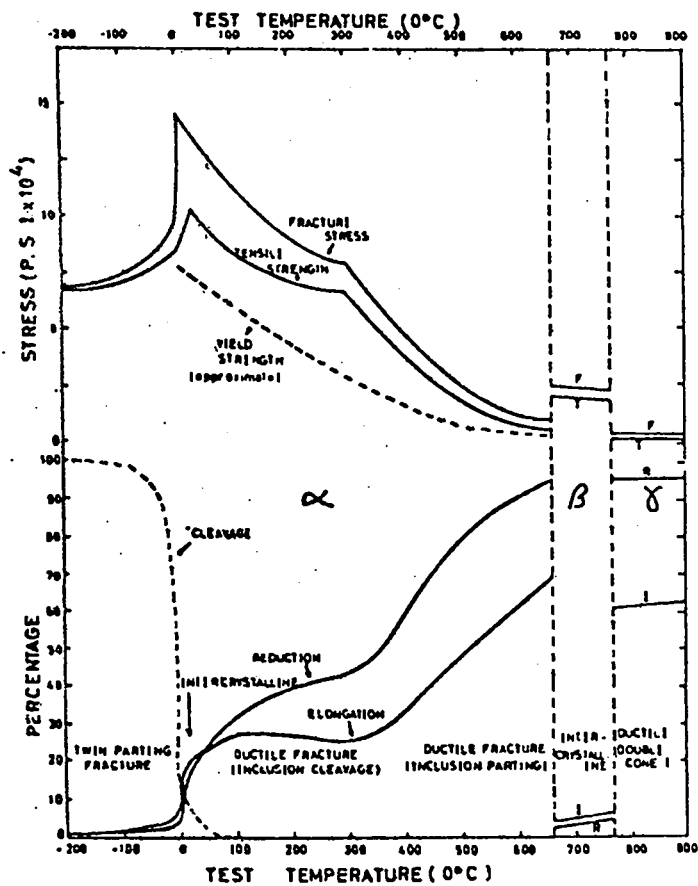


75X

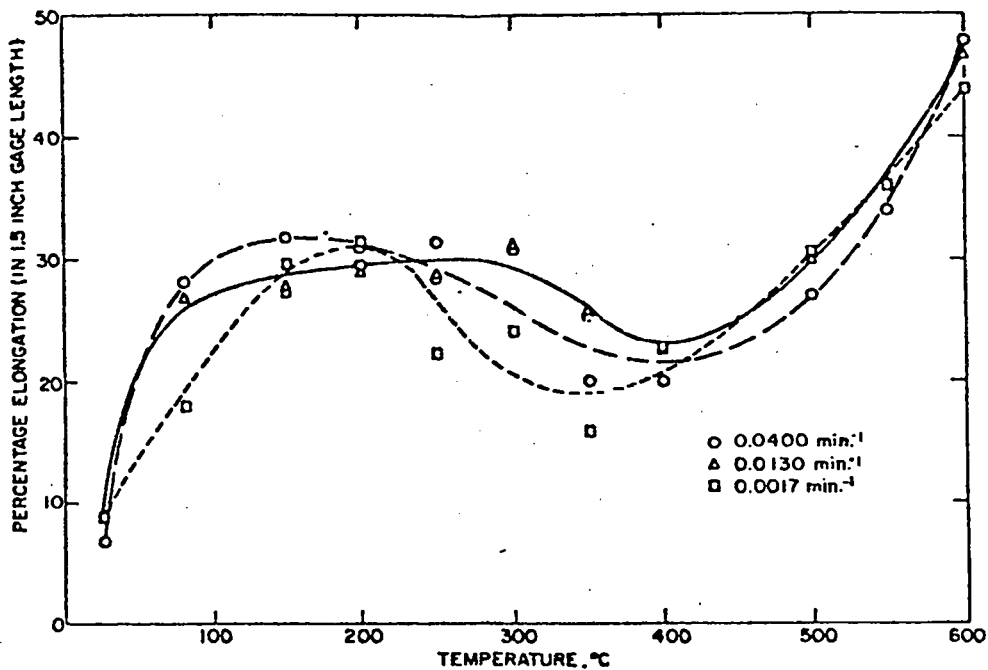


75X

Fig. 21. SEM photographs of Y-12 sheet CM 3 8480 round tensile specimen after testing at 25°C at a strain rate of $6.7 \times 10^{-4} \text{ s}^{-1}$. "B" direction. Top: Fracture surface. Bottom: Cylindrical surface showing relative freedom from circumferential cracks.



The effect of test temperature (-200°C to $+900^{\circ}\text{C}$) on the tensile properties and fracture of uranium.



Per Cent Elongation as Function of Temperature for Three Different Strain Rates.

Fig. 22. Mechanical properties of uranium at slow strain rates. Upper graph from ref. 4. Lower graph from ref. 5.

The high temperature tests have some interesting implications in shaped-charge performance. Since the strength and ductilities differ considerably and perhaps discontinuously over a temperature range of 250°C, the total internal energy in the system becomes extremely important. Either a small increase or a small decrease can bring the temperature into the beta phase region where the strengths and ductilities have been reported to differ substantially and might account for the variability in reproducibility of results occasionally observed.

9.3 Effect of Hydrogen

Not enough high strain rate tests have been conducted on these uranium materials to allow a conclusive determination of the effect of very small amounts of hydrogen on the ductility at high strain rates. However, liners that were vacuum annealed at 625°C have been fired from the CM 3 8480 material and had a hydrogen content of 0.19 ppm, from 69702 material with hydrogen contents of 0.14 (vacuum annealed at 625°C) and 1.7 ppm (vacuum annealed at 400°C). The CM 3 8480 material performed the best with all of the 69073 material somewhat poorer. There was very little difference in the performance of the 69072 material containing 0.8 or 1.7 ppm hydrogen - if any the 0.8 ppm material was better. Another liner of 69072 material, that had been given a different annealing treatment, contained 0.14 ppm hydrogen and it performed no better than those containing more hydrogen. This data certainly indicates that very low < 1 ppm, ppm hydrogen contents may not be required for liner applications. However, the data are limited and it will be necessary to examine high strain rate data and additional liner data before firm conclusions can be drawn.

References

1. Dickinson J.M. Armor Defeat Mechanism, Alternative Materials Selection February - April 1980 LA 8413 PR, Los Alamos Scientific Laboratory (1980).
2. Robinson S.L., Sherby O.D. and Armstrong P.E. J. Nucl Mat'er 46 (1973) 293.
3. Franz C.E. and Hecker S.S. High Rate Mechanical Testing with the LASL Two-Inch Gun. LA 6528 Los Alamos Scientific Laboratory (1976).
4. Taplin D.M.R., J. Austr Inst. Metals 12 (1967) 32-44.
5. Loretan D.A. and Murphy G. Proc. Amer. Soc. Testing Mater. 64 (1964) 734-46.

Printed in the United States of America
 Available from
 National Technical Information Service
 US Department of Commerce
 5285 Port Royal Road
 Springfield, VA 22161
 Microfiche \$3.50 (A01)

Page Range	Domestic Price	NTIS Price Code	Page Range	Domestic Price	NTIS Price Code	Page Range	Domestic Price	NTIS Price Code	Page Range	Domestic Price	NTIS Price Code
001-025	\$ 5.00	A02	151-175	\$11.00	A08	301-325	\$11.00	A14	451-475	\$23.00	A20
026-050	6.00	A03	176-200	12.00	A09	326-350	13.00	A15	476-500	24.00	A21
051-075	7.00	A04	201-225	13.00	A10	351-375	14.00	A16	501-525	25.00	A22
076-100	8.00	A05	226-250	14.00	A11	376-400	15.00	A17	526-550	26.00	A23
101-125	9.00	A06	251-275	15.00	A12	401-425	16.00	A18	551-575	27.00	A24
126-150	10.00	A07	276-300	16.00	A13	426-450	17.00	A19	576-600	28.00	A25
									601-up	†	A99

† Add \$1.00 for each additional 25-page increment or portion thereof from 601 pages up.

LOS ALAMOS
REPORT LIBRARY

AUG -3 1982

RECEIVED